Observations of Space Object 2020 SO Using 8-inch f/2 Schmidt Astrograph

Tim McLaughlin
Pine Park Engineering Corporation
Roger L. Mansfield
The MITRE Corporation

ABSTRACT

Using a Schmidt astrograph of 8" (0.2m) aperture and f/2 focal ratio, the space object designated as 2020 SO was acquired and tracked prior to its perigee of 2021 February 2. Acquisition occurred at approximately 283,800 km range (44.5 Earth radii) on February 1. This paper documents the detection, acquisition, tracking, metric and photometric data collection, and data reduction for seemingly-asteroidal object 2020 SO's latest entry into cislunar space.

1. INTRODUCTION

The International Astronomical Union's Minor Planet Center (MPC) reported, in electronic circular MPEC 2020-S78 dated 2020 September 19, that the Mt. Haleakala observatories Pan-STARRS2 and Pan-STARRS1, and the Catalina Sky Survey's Kuiper Observatory had all tracked an apparently asteroidal object, now designated as 2020 SO.

Due to its low velocity relative to Earth, 2020 SO was thought maybe to be an artificial object. When it became possible to further investigate the orbit and ephemeris (e.g., via the JPL Horizons website), it was evident that the object had entered Earth's cislunar regime on 2020 December 1 and would do so again on 2021 February 2 (see the Wikipedia entry for 2020 SO).

Fig. 1 depicts both 2020 SO's 2020 December 1 perigee and its 2021 February 2 perigee. The snapshot captures 2020 SO right before its 2021 February 2 perigee. The light-colored circle depicts Moon's orbit around Earth.

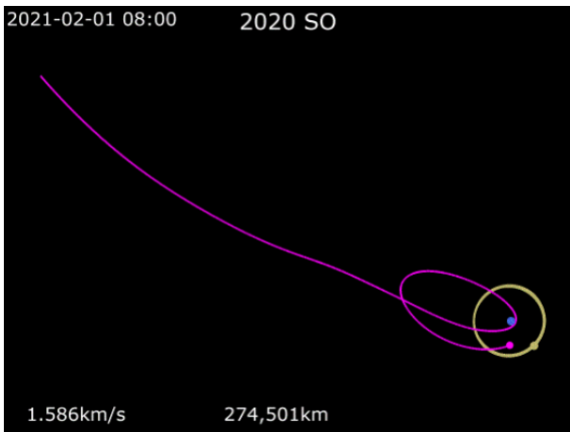

Fig. 1. Snapshot of Wikipedia animation of 2020 SO's path (red) around Earth (blue dot).
Source: https://en.wikipedia.org/wiki/2020_SO

Following 2020 SO's close passage on 2020 December 1, interest in the object grew because a) its origin was uncertain, b) it had entered cislunar space quite close to Earth on that date, and c) it would enter cislunar space again two months later, close to Earth but not so close as before.

It had been determined, via reconstruction of the past trajectory (by Paul Chodas of NASA's Jet Propulsion Laboratory), that 2020 SO is likely the Centaur rocket booster from the Surveyor 2 launch in 1966. Spectroscopic

observations by NASA's Infrared Telescope Facility in December 2020 indicated that 2020 SO's spectrum is similar to that of stainless steel. The spectral evidence, together with trajectory reconstruction efforts, have led to a consensus that object 2020 SO likely originated from Earth in 1966.

That which enters cislunar space is of interest to the space community from the perspectives of both space situational awareness (SSA) and space domain awareness (SDA). How big, how expensive must an observatory be to be useful for the surveillance of cislunar space?

To demonstrate that small, optically-fast but relatively-inexpensive telescopes can be advantageous for this purpose, we decided to attempt to track 2020 SO right before its 2021 February 2 perigee. Our AMOS 2021 paper is about our success here.

2. TELESCOPE SYSTEM HARDWARE AND SOFTWARE

The Pine Park Observatory (PPO, Colorado) presently has two 8-inch-aperture telescopes, the f/2 Celestron Rowe-Ackermann Schmidt Astrograph (the "RASA") and an f/6.3 Celestron Schmidt-Cassegrain telescope. The RASA, having much higher etendue [1], was selected for tracking space object 2020 SO.

Figs. 2a and 2b. RASA and Mount Configuration for the Pine Park Observatory.

Figs. 2a and 2b illustrate the RASA and its mount. The optical tube assembly (OTA) is secured to the Celestron CGX-L German equatorial mount via a dovetail. (The dovetail is the long orange plate. It spans almost the length of the OTA.) A QHY-174M-GPS camera is mounted on the corrector lens assembly. The corrector lens assembly itself is attached to the Schmidt corrector plate at the front of the OTA.

Telescope control was accomplished using a custom telescope control program. The program supports multiple tracking modes (both rate-tracking and sidereal). For typical Earth-orbiting satellites, a Two-Line Element Set (TLE) is used to drive the telescope in rate-tracking mode. In this mode, the telescope will follow the satellite and the stars will streak through the field of view (FOV). Due to the great distance of 2020 SO as an "Earth satellite" moving against the star background, rate-tracking was slow: the target moved relatively little during the almost six-hour tracking period.

For rate track, the image is first processed with the Source Extractor software to find the centroid of each star streak. The centroid points are assembled into a binary table representing the xy positions of stars in the FOV. The binary table is passed along to the Astrometry.net software to register the xy positions to the star field. The software returns the exact coordinates (RA and DEC) of the center of the image and a plate model. Aberration corrections are then applied to the RA and DEC J2000 coordinate measurements before referring them to the true equator and mean equinox of date to feed the orbit determination process.

3. TRACKING AND MEASUREMENTS

We used the JPL Horizons website [2] to generate predictions of the visibility of space object 2020 SO to the PPO Observatory during the night of 2021 February 1 UTC. Using these predictions, we had no trouble finding 2020 SO. The PPO collected 129 metric observations of 2020 SO. These topocentric time, right ascension (**RA-HRMNSEC**), and declination (**ELDEC**) measurements can be found in the Appendix, together with the latitude, longitude, and height-above-mean-sea level of the PPO.

The PPO Observatory also made photometric measurements. They are plotted below in Fig. 3.

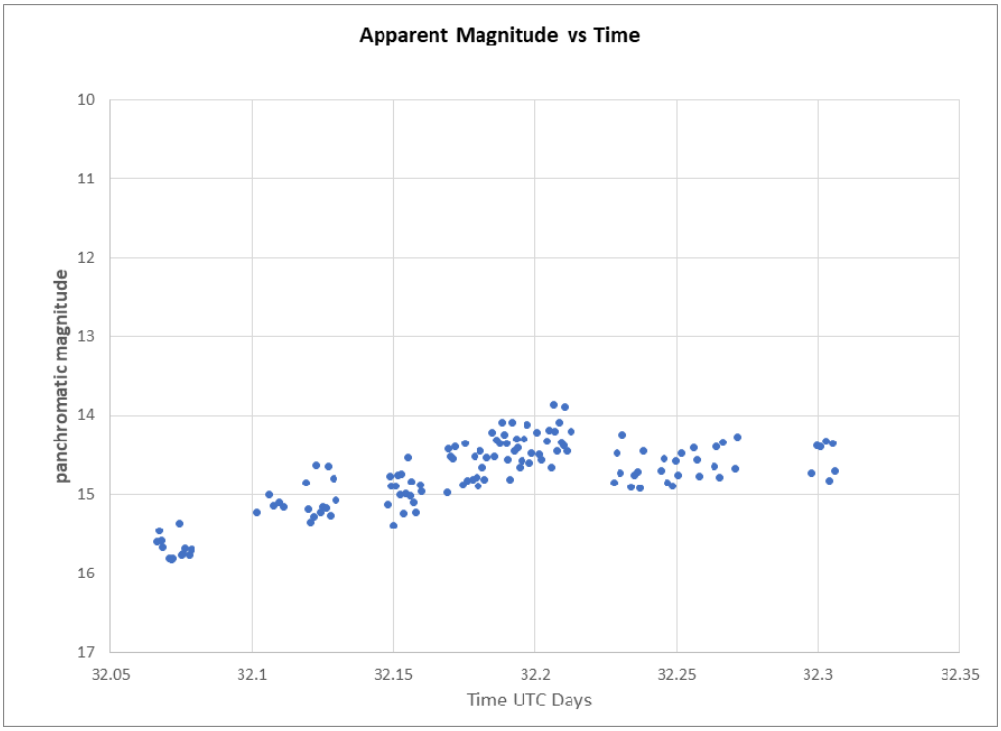

Fig. 3. Panchromatic photometry measurements of space object 2020 SO made on 2021 February 1 UTC.

Sunset occurred at the PPO at about 00:19 UTC on 2021 February 1 (17:19 MST on January 31). The night sky was devoid of sunlight during the entire period of observation of 2020 SO, i.e., from 01:36 to 07:20 UTC on February 1 (18:36 to 24:20 MST on January 31).

Moonrise occurred at about 03:44 UTC on February 1 (20:44 MST on January 31), with the Moon rising at about 87 % illumination. Although the Moon's phase was three nights past full, the Moon was so situated in the night sky that it did not interfere with the PPO's observation of 2020 SO.

During the six-hour span of observations, the apparent magnitude of 2020 SO varied between 15.7 (fainter) and 14.0 brighter). Likewise, solar phase angle varied from 11.36 to 10.8 degrees. (Full illumination corresponds to zero degrees of phase angle.)

An mp4 video was recorded during the rate-tracking of 2020 SO. Fig. 4 is a labeled snapshot from the mp4 video. As noted in the previous section, during rate-track the stars streak as the telescope tracks the target. This can be clearly seen in the snapshot.

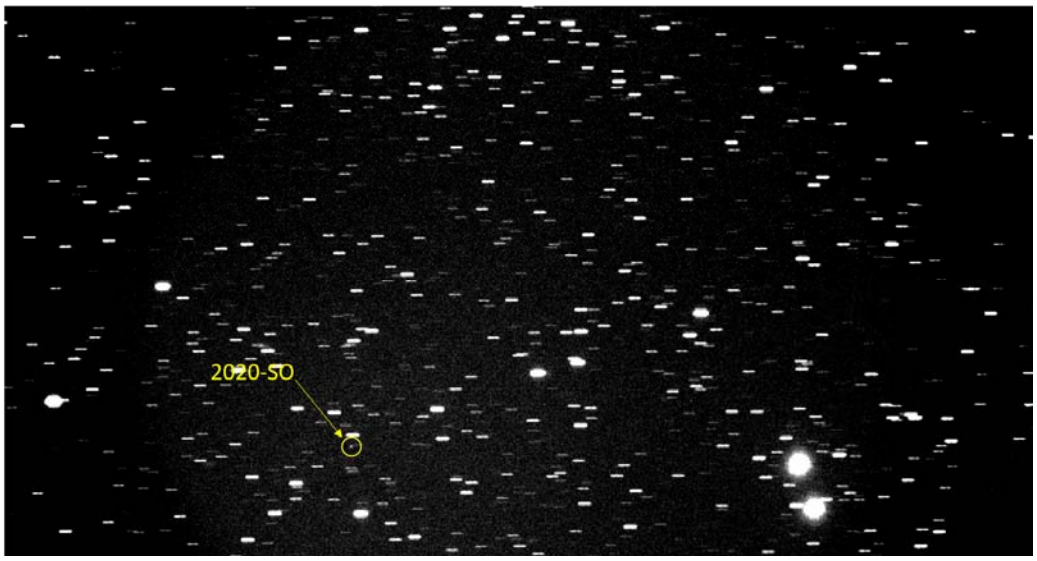

Fig. 4. Snapshot of mp4 video taken by PPO Observatory as the RASA-based electro-optical system tracked cislunar space object 2020 SO. Arrow points to circle around 2020 SO.

4. METRIC MEASUREMENTS REDUCTION

We used the Gauss [3], Laplace [4], and HGM [5] initial orbit determination (IOD) methods with PPO observations 1, 60, and 129 (see again Appendix) to generate preliminary orbits for input to the Batch UPM DC method, BDC. The solutions are tabulated in Table 1.

Table 1. Gauss, Laplace, and HGM IOD Solutions with PPO Observations 1, 60, and 129.

Orbital Element	Gauss Method Solution	Laplace Method Solution	HGM Method Solution
Semimajor axis, ER	145.79143567	140.39403369	149.99408307
Eccentricity	0.76295389	0.75345021	0.75882854
Inclination, deg	29.42189	29.44108	29.38826
Rt. Asc. of Asc. Node, deg	27.45917	27.30263	27.67986
Arg. of Perigee, deg	164.20589	164.50320	159.69244
Mean Anomaly, deg	353.79707	353.38769	354.65409
Mean Motion, rev/day	0.00968198	0.01024564	0.00927792
Period, days	103.2847	97.6025	107.7827

Note: Epochs of Gauss and Laplace solutions are at time of observation 60. Epoch of HGM solution is at time of observation 129 (last observation).

Given that HGM is a preliminary orbit determination method that can work with all available observations (subject to a geocentric arc span limitation – see again [5]), Table 2 shows the results when all 129 observations are input to HGM and to BDC. Note, as documented in [6], [7], and [8], that BDC is a DC based upon the universal-variables, two-body path propagation theory known as Uniform Path Mechanics (UPM).

Since BDC is a two-body DC, the solution obtained, using 129 observations distributed over a time span of almost six hours, is a good approximation to an osculating solution. It represents the elliptical, Earth-captured path that 2020 SO would have continued along, were it not for significant gravitational perturbations by the Moon and Sun.

Now, which of the three preliminary orbit determination methods cited in Table 1 is the best? The Gauss and Laplace methods will work when all three observations are spread out over an entire orbital revolution, whereas HGM is a so-called “short-arc” method: it is good when an “actionable” orbit is needed as soon as sufficient tracking has taken place. All three are good enough to initiate a batch DC such as BDC. The Gauss and Laplace

solutions, when input to BDC, needed four iterations for the BDC DC to converge, whereas the HGM solution, when input to BDC, needed only two. But this is because HGM solution has epoch at the time of the last observation, same as BDC, whereas the Gauss and Laplace solutions have epoch at the middle observation. Two more iterations were needed with Gauss and Laplace to, in effect, move epoch from the time of the middle observation to the time of the last observation.

Table 2. HGM and BDC Solutions with all 129 PPO Observations.

Orbital Element or Parameter	HGM Method Solution	BDC DC Solution
Semimajor axis, ER	149.89890322	136.88449775
Eccentricity	0.75975092	0.73700902
Inclination, deg	29.38888	29.39303
Rt. Asc. of Asc. Node, deg	27.67796	27.65155
Arg. of Perigee, deg	160.11643	160.25614
Mean Anomaly, deg	354.63105	353.80872
Mean Motion, rev/day	0.00928676	0.01064218
Period, days	107.6802	93.9657
RMS Error, km	6.238	0.131

Note: Epochs of HGM and BDC solutions are at time of observation 129 (last observation).

One could assert that the BDC solution is not truly an osculating solution, given that it is the result of a DC with observations spread out over almost six hours. But given, as is shown in Table 2, that the orbital period is almost 94 days, we can see that a six-hour observation span corresponds to 0.25 days / 94 days = 0.00266, or about 0.27 % of a full elliptical orbit.

Indeed, space object 2020 SO was a rare occurrence in the cislunar regime in the year 2020. As with a natural body, it was not thrusting, and it appeared at the time of tracking to be in Earth capture. But we can easily see from the Wikipedia animation of the perturbed path (only a snapshot of which was depicted in Fig.1), that 2020 SO was not in fact in Earth capture.

We decided to further investigate the cislunar orbital behavior of 2020 SO by going to the JPL Horizons website again, but now to generate the JPL Horizons ephemeris over six hours that overlap the time interval during which we tracked 2020 SO. We converted each position and velocity in the JPL ephemeris to classical elements. Table 3 shows the results of this “truly osculating” orbital elements ephemeris.

Since the first PPO observation took place at 1:35:47.426 UTC, linear interpolation between the geocentric distances in the table yields about 0.579 x (290,034 – 290,445) = -238. Now 290,445 – 238 = 290,207 km. Subtracting one Earth radius, about 6378 km, from this result yields an approximate range of 283,829 km, or about 44.5 Earth radii, the distance at acquisition reported in this paper’s abstract.

Table 3 further shows that 2020 SO’s geocentric orbital eccentricity during the PPO tracking period was steadily increasing toward a value greater than unity, i.e., Earth escape, and that its geocentric distance was steadily decreasing as 2020 SO advanced toward its perigee of 2021 February 2.

We should note that the time column in Table 3 is not UTC, but rather Barycentric Dynamical Time (TDB). TDB is a time scale better suited than UTC for modeling the motions of natural bodies in the solar system [9, p. M3] and [10]. Whereas Coordinated Universal Time (UTC) is better suited for space operations that deal with the motions of spacecraft in Earth orbit [9, p. M4]. In 2020-2021, UTC equals TDB minus about 70 seconds [9, p. K9].

Table 3. Osculating Orbital Elements Ephemeris for Space Object 2020 SO.

TDB hr:min	Mean Motion rev/day	Eccen-tricity	Inclinatn. deg	Rt.Ascen. A.N. deg	Arg.Per. deg	Mean Anom., deg	Geocentric Dist., km	Geocentric Dist,. ER
1:30	0.00808285	0.7857657	29.4483	27.5588	161.8483	354.5792	290444.698	45.537550
1:40	0.00808065	0.7858021	29.4484	27.5581	161.8467	354.6010	290034.208	45.473191
1:50	0.00807844	0.7858387	29.4484	27.5575	161.8451	354.6229	289624.368	45.408934
2:00	0.00807623	0.7858754	29.4485	27.5568	161.8435	354.6448	289215.183	45.344779
2:10	0.00807401	0.7859122	29.4486	27.5561	161.8418	354.6666	288806.660	45.280729
2:20	0.00807178	0.7859492	29.4486	27.5555	161.8402	354.6885	288398.803	45.216783
2:30	0.00806955	0.7859862	29.4487	27.5548	161.8386	354.7103	287991.617	45.152942
2:40	0.00806731	0.7860234	29.4488	27.5541	161.8370	354.7322	287585.109	45.089207
2:50	0.00806506	0.7860607	29.4488	27.5535	161.8354	354.7540	287179.283	45.025580
3:00	0.00806281	0.7860981	29.4489	27.5528	161.8337	354.7759	286774.146	44.962060
3:10	0.00806055	0.7861357	29.4490	27.5521	161.8321	354.7977	286369.702	44.898649
3:20	0.00805829	0.7861733	29.4490	27.5515	161.8305	354.8195	285965.957	44.835347
3:30	0.00805601	0.7862111	29.4491	27.5508	161.8289	354.8413	285562.917	44.772157
3:40	0.00805373	0.7862491	29.4492	27.5501	161.8272	354.8631	285160.587	44.709077
3:50	0.00805145	0.7862871	29.4493	27.5495	161.8256	354.8849	284758.973	44.646110
4:00	0.00804916	0.7863253	29.4494	27.5488	161.8240	354.9067	284358.081	44.583256
4:10	0.00804686	0.7863636	29.4494	27.5481	161.8223	354.9284	283957.916	44.520515
4:20	0.00804455	0.7864021	29.4495	27.5474	161.8207	354.9502	283558.483	44.457890
4:30	0.00804223	0.7864407	29.4496	27.5468	161.8190	354.9720	283159.790	44.395381
4:40	0.00803991	0.7864794	29.4497	27.5461	161.8174	354.9937	282761.841	44.332988
4:50	0.00803758	0.7865183	29.4498	27.5454	161.8157	355.0155	282364.642	44.270713
5:00	0.00803525	0.7865573	29.4498	27.5447	161.8141	355.0372	281968.200	44.208557
5:10	0.00803290	0.7865964	29.4499	27.5441	161.8124	355.0590	281572.519	44.146520
5:20	0.00803055	0.7866357	29.4500	27.5434	161.8108	355.0807	281177.606	44.084603
5:30	0.00802819	0.7866751	29.4501	27.5427	161.8091	355.1024	280783.467	44.022808
5:40	0.00802583	0.7867147	29.4502	27.5420	161.8075	355.1241	280390.108	43.961135
5:50	0.00802345	0.7867544	29.4503	27.5414	161.8058	355.1458	279997.534	43.899585
6:00	0.00802107	0.7867942	29.4504	27.5407	161.8041	355.1675	279605.752	43.838159
6:10	0.00801868	0.7868342	29.4505	27.5400	161.8025	355.1892	279214.768	43.776858
6:20	0.00801629	0.7868743	29.4506	27.5393	161.8008	355.2109	278824.588	43.715683
6:30	0.00801388	0.7869146	29.4507	27.5386	161.7991	355.2326	278435.217	43.654636
6:40	0.00801147	0.7869551	29.4508	27.5380	161.7975	355.2543	278046.663	43.593716
6:50	0.00800905	0.7869957	29.4509	27.5373	161.7958	355.2759	277658.930	43.532925
7:00	0.00800662	0.7870364	29.4510	27.5366	161.7941	355.2976	277272.027	43.472264
7:10	0.00800418	0.7870773	29.4511	27.5359	161.7924	355.3193	276885.957	43.411734
7:20	0.00800173	0.7871184	29.4512	27.5352	161.7907	355.3409	276500.729	43.351336
7:30	0.00799928	0.7871596	29.4513	27.5345	161.7890	355.3625	276116.348	43.291070

5. SUMMARY AND CONCLUSION

This paper has documented the detection, acquisition, tracking, metric and photometric data collection, and data reduction for the seemingly-asteroidal (but actually man-made) object 2020 SO's latest entry into cislunar space.

The IOD and DC results with the 129 observations collected just before 2020 SO's perigee of 2021 February 2 demonstrate that small-aperture, but optically-fast telescopes of high etendue can advantageously track faint cislunar objects, e.g., asteroids and man-made objects entering cislunar space, to include space probe launches and flybys and artificial Earth satellites in multi-day orbits with distant apogees.

6. ACKNOWLEDGMENTS

We would like to thank Mr. Scott Wacker of MITRE Los Angeles (El Segundo) for urging us to track 2020 SO, on account of the great interest in this space object as exhibited in 2020-2021 by the dynamical astronomy, civil space, and military space communities. We would also like to thank Dr. Gim J. Der of Der Astrodynamics for helping us to verify the Gauss and Laplace IOD solutions, and the BDC solution with 129 observations.

7. REFERENCES

[1] Richard Berry and Celestron Engineering Team, “Big! Fast! Wide! Sharp! The Story of the Celestron Rowe-Ackermann Schmidt Astrograph,” © 2016 by Celestron, 2835 Columbia Street, Torrance, CA 90503 USA.

[2] HORIZONS Web-Interface, JPL’s HORIZONS System https://ssd.jpl.nasa.gov/horizons.cgi.

[3] Howard D. Curtis, *Orbital Mechanics for Engineering Students* (Elsevier, Second Edition 2009), Section 5.10, Gauss method of preliminary orbit determination. Algorithm 5.5.

[4] Pedro R. Escobal, *Methods of Orbit Determination,* (Krieger Publishing Company, Malabar, Florida, reprint 1976 w/corrections of original First edition, John Wiley & Sons, Inc. 1965), Section 7.4, The Method of Laplace.

[5] Roger L. Mansfield, “Preliminary Determination of the Geocentric Earth Flyby Path of Asteroid 2012 DA14,” AAS Paper 14-288, *24th AAS/AIAA Space Flight Mechanics Meeting,* Santa Fe, New Mexico, 28 January 2014.

[6] Roger L. Mansfield and Gim J. Der, "Reconstruction of the 1801 Discovery Orbit of Ceres via Contemporary Angles-Only Algorithms," *Advanced Maui Optical and Space Surveillance Technologies (AMOS) Conference 2016*, Maui, Hawaii USA, 20-23 September 2016.

[7] Roger L. Mansfield and Tim McLaughlin, “MITRE Telescope Tracks BepiColombo Flyby,” AAS Paper 20-537, *AAS/AIAA Astrodynamics Specialist Virtual Lake Tahoe Conference,* August 9-13, 2020.

[8] Roger L. Mansfield, *Topics in Astrodynamics,* Astronomical Data Service, Colorado Springs, Colorado USA, February 2003. http://astrotopics.astroger.com. Chapters 14 and 15.

[9] Nautical Almanac Office, U.S. Naval Observatory and Her Majesty’s Nautical Almanac Office, United Kingdom, *The Astronomical Almanac for the Year 2021,* Washington, DC USA and Taunton, UK, Sections K, L, and M.

[10] Sean E. Urban and P. Kenneth.Seidelmann (Editors), *Explanatory Supplement to the Astronomical Almanac,* University Science Books, Third Edition (2013), Mill Valley, California USA.

8. APPENDIX

BDC DC output summary, bdc_sum.txt, for DC with 129 PPO observations of 2020 SO, is given below.

Table A1. Batch UPM DC Output Summary for Space Object 2020 SO.

BATCH UPM DIFFERENTIAL CORRECTION PROGRAM (BDC)

THETA-G AT JAN 0.0 UTC, FROM HGM_SEN.TXT: 99.88310

SENSOR DATA FOR 1 SENSOR:

SEN	LAT	LONG	HKM
284	38.99428	-104.640980	2.2500

INITIAL ESTIMATE OF X, KM	-179493.184
INITIAL ESTIMATE OF Y, KM	166786.051
INITIAL ESTIMATE OF Z, KM	130145.320
INITIAL ESTIMATE OF XDOT, KM/SEC	-0.662479768
INITIAL ESTIMATE OF YDOT, KM/SEC	-1.332699372
INITIAL ESTIMATE OF ZDOT, KM/SEC	-0.491408521

SUMMARY OF OBSERVATIONS INPUT:

SATNO	SEN	YY	DDD	HH	MM	SS.SSS	ELDEC	RA-HRMNSEC	NBR
70000	284	21	32	1	35	47.426	28.1631	8 46 13.0	1
70000	284	21	32	1	36	47.421	28.1631	8 46 17.3	2
70000	284	21	32	1	37	47.416	28.1630	8 46 21.3	3
70000	284	21	32	1	38	47.409	28.1629	8 46 25.9	4
70000	284	21	32	1	41	47.398	28.1628	8 46 38.6	5
70000	284	21	32	1	42	47.389	28.1628	8 46 43.0	6
70000	284	21	32	1	43	47.381	28.1628	8 46 47.2	7
70000	284	21	32	1	46	47.364	28.1625	8 47 0.3	8
70000	284	21	32	1	47	47.361	28.1626	8 47 4.4	9
70000	284	21	32	1	48	47.355	28.1626	8 47 8.6	10
70000	284	21	32	1	49	47.348	28.1624	8 47 12.9	11
70000	284	21	32	1	51	47.336	28.1622	8 47 21.5	12
70000	284	21	32	1	52	47.332	28.1624	8 47 25.7	13
70000	284	21	32	2	26	37.617	28.1568	8 49 47.7	14
70000	284	21	32	2	32	37.583	28.1553	8 50 12.2	15
70000	284	21	32	2	34	37.573	28.1548	8 50 20.8	16
70000	284	21	32	2	37	37.555	28.1533	8 50 33.0	17
70000	284	21	32	2	39	37.545	28.1527	8 50 41.1	18
70000	284	21	32	2	51	37.475	28.1489	8 51 30.2	19
70000	284	21	32	2	52	37.471	28.1485	8 51 34.4	20
70000	284	21	32	2	53	37.464	28.1479	8 51 38.2	21
70000	284	21	32	2	55	37.454	28.1472	8 51 46.4	22
70000	284	21	32	2	56	37.450	28.1466	8 51 50.4	23
70000	284	21	32	2	58	37.438	28.1460	8 51 58.4	24
70000	284	21	32	2	59	37.432	28.1455	8 52 2.4	25
70000	284	21	32	3	1	37.421	28.1446	8 52 10.4	26
70000	284	21	32	3	2	37.414	28.1438	8 52 14.5	27
70000	284	21	32	3	3	37.408	28.1436	8 52 18.6	28
70000	284	21	32	3	5	37.398	28.1423	8 52 26.8	29
70000	284	21	32	3	6	37.391	28.1418	8 52 30.6	30
70000	284	21	32	3	33	5.538	28.1264	8 54 16.1	31
70000	284	21	32	3	34	5.535	28.1260	8 54 20.0	32
70000	284	21	32	3	35	5.529	28.1253	8 54 24.0	33
70000	284	21	32	3	36	5.524	28.1244	8 54 27.9	34
70000	284	21	32	3	37	5.518	28.1240	8 54 31.7	35
70000	284	21	32	3	38	5.513	28.1233	8 54 35.8	36
70000	284	21	32	3	39	5.506	28.1223	8 54 39.7	37
70000	284	21	32	3	40	5.501	28.1220	8 54 43.6	38
70000	284	21	32	3	41	5.494	28.1211	8 54 47.5	39
70000	284	21	32	3	42	5.488	28.1200	8 54 51.2	40
70000	284	21	32	3	43	5.485	28.1196	8 54 55.2	41
70000	284	21	32	3	44	5.479	28.1184	8 54 59.3	42
70000	284	21	32	3	45	5.471	28.1176	8 55 3.0	43

SATNO	SEN	YY	DDD	HH	MM	SS.SSS	ELDEC	RA-HRMNSEC	NBR
70000	284	21	32	3	46	5.466	28.1173	8 55 7.1	44
70000	284	21	32	3	47	5.459	28.1160	8 55 10.8	45
70000	284	21	32	3	49	5.449	28.1146	8 55 18.9	46
70000	284	21	32	3	50	5.446	28.1135	8 55 22.3	47
70000	284	21	32	4	3	5.372	28.1021	8 56 13.1	48
70000	284	21	32	4	4	5.367	28.1016	8 56 16.7	49
70000	284	21	32	4	5	5.360	28.1006	8 56 20.8	50
70000	284	21	32	4	6	5.355	28.1005	8 56 24.7	51
70000	284	21	32	4	7	5.348	28.0987	8 56 28.5	52
70000	284	21	32	4	11	5.328	28.0945	8 56 43.6	53
70000	284	21	32	4	12	5.322	28.0935	8 56 47.5	54
70000	284	21	32	4	13	5.315	28.0924	8 56 51.6	55
70000	284	21	32	4	16	5.299	28.0900	8 57 3.3	56
70000	284	21	32	4	17	5.294	28.0880	8 57 6.6	57
70000	284	21	32	4	18	5.290	28.0870	8 57 10.7	58
70000	284	21	32	4	19	5.284	28.0858	8 57 14.5	59
70000	284	21	32	4	20	5.278	28.0850	8 57 18.2	60
70000	284	21	32	4	21	5.271	28.0860	8 57 22.8	61
70000	284	21	32	4	22	5.267	28.0831	8 57 25.8	62
70000	284	21	32	4	23	5.260	28.0817	8 57 29.8	63
70000	284	21	32	4	26	5.245	28.0781	8 57 41.3	64
70000	284	21	32	4	27	5.239	28.0782	8 57 45.2	65
70000	284	21	32	4	28	5.231	28.0757	8 57 48.6	66
70000	284	21	32	4	30	5.223	28.0738	8 57 56.2	67
70000	284	21	32	4	31	5.216	28.0725	8 58 0.2	68
70000	284	21	32	4	32	5.210	28.0721	8 58 4.2	69
70000	284	21	32	4	33	5.207	28.0701	8 58 7.6	70
70000	284	21	32	4	34	5.199	28.0694	8 58 11.8	71
70000	284	21	32	4	35	5.194	28.0692	8 58 15.6	72
70000	284	21	32	4	36	5.187	28.0661	8 58 18.9	73
70000	284	21	32	4	37	5.182	28.0665	8 58 23.5	74
70000	284	21	32	4	38	5.178	28.0642	8 58 26.6	75
70000	284	21	32	4	39	5.173	28.0628	8 58 30.5	76
70000	284	21	32	4	40	5.167	28.0614	8 58 34.2	77
70000	284	21	32	4	41	5.162	28.0605	8 58 37.8	78
70000	284	21	32	4	42	5.156	28.0585	8 58 41.8	79
70000	284	21	32	4	44	5.144	28.0567	8 58 49.3	80
70000	284	21	32	4	45	5.138	28.0559	8 58 53.4	81
70000	284	21	32	4	46	5.132	28.0538	8 58 56.8	82
70000	284	21	32	4	49	5.118	28.0502	8 59 8.1	83
70000	284	21	32	4	50	5.109	28.0492	8 59 12.2	84
70000	284	21	32	4	51	5.104	28.0471	8 59 15.5	85
70000	284	21	32	4	54	5.087	28.0435	8 59 27.0	86
70000	284	21	32	4	55	5.085	28.0415	8 59 30.9	87
70000	284	21	32	4	56	5.076	28.0402	8 59 34.5	88
70000	284	21	32	4	57	5.072	28.0391	8 59 38.2	89
70000	284	21	32	4	58	5.067	28.0372	8 59 42.1	90
70000	284	21	32	4	59	5.060	28.0360	8 59 45.7	91
70000	284	21	32	5	0	5.055	28.0344	8 59 49.4	92
70000	284	21	32	5	1	5.050	28.0328	8 59 53.3	93
70000	284	21	32	5	2	5.045	28.0315	8 59 56.9	94
70000	284	21	32	5	3	5.039	28.0296	9 0 0.9	95
70000	284	21	32	5	4	5.034	28.0283	9 0 4.3	96
70000	284	21	32	5	6	5.023	28.0251	9 0 12.1	97
70000	284	21	32	5	27	56.187	27.9901	9 1 31.5	98
70000	284	21	32	5	29	26.186	27.9877	9 1 36.6	99
70000	284	21	32	5	30	56.185	27.9847	9 1 42.4	100
70000	284	21	32	5	32	26.184	27.9821	9 1 48.0	101
70000	284	21	32	5	36	56.180	27.9738	9 2 4.4	102
70000	284	21	32	5	38	26.177	27.9713	9 2 10.3	103
70000	284	21	32	5	39	56.177	27.9685	9 2 15.3	104
70000	284	21	32	5	41	26.176	27.9654	9 2 21.2	105
70000	284	21	32	5	42	56.175	27.9627	9 2 26.5	106
70000	284	21	32	5	51	56.165	27.9447	9 3 0.0	107
70000	284	21	32	5	53	26.164	27.9423	9 3 5.1	108
70000	284	21	32	5	54	56.162	27.9391	9 3 10.6	109
70000	284	21	32	5	57	56.160	27.9327	9 3 21.9	110

SATNO	SEN	YY	DDD	HH	MM	SS.SSS	ELDEC	RA-HRMNSEC	NBR
70000	284	21	32	5	59	26.160	27.9294	9 3 27.6	111
70000	284	21	32	6	0	56.158	27.9266	9 3 32.7	112
70000	284	21	32	6	2	26.157	27.9231	9 3 38.6	113
70000	284	21	32	6	8	26.151	27.9105	9 4 0.3	114
70000	284	21	32	6	9	56.150	27.9071	9 4 6.0	115
70000	284	21	32	6	11	26.149	27.9040	9 4 11.1	116
70000	284	21	32	6	18	56.141	27.8867	9 4 38.9	117
70000	284	21	32	6	20	26.140	27.8831	9 4 44.4	118
70000	284	21	32	6	21	56.140	27.8790	9 4 50.0	119
70000	284	21	32	6	23	26.138	27.8762	9 4 55.4	120
70000	284	21	32	6	29	26.132	27.8614	9 5 17.3	121
70000	284	21	32	6	30	56.130	27.8584	9 5 22.8	122
70000	284	21	32	7	8	26.098	27.7579	9 7 40.0	123
70000	284	21	32	7	11	26.094	27.7491	9 7 51.1	124
70000	284	21	32	7	12	56.095	27.7450	9 7 56.2	125
70000	284	21	32	7	15	56.093	27.7362	9 8 7.3	126
70000	284	21	32	7	17	26.089	27.7314	9 8 13.0	127
70000	284	21	32	7	18	56.091	27.7269	9 8 18.6	128
70000	284	21	32	7	20	26.086	27.7225	9 8 23.9	129

THETA-G (DEG) AT JAN 0.0 UTC OF TLOB YEAR 2021 = 99.88310

ITER = 0 WRMS = 0.144 PWRMS = 0.131
ITER = 1 WRMS = 0.131 PWRMS = 0.131

CONVERGED BY CRITERION 2. EPS2 = 0.010

STATE VECTOR SOLUTION AT EPOCH:

X, KM	-178926.890861
Y, KM	166276.312111
Z, KM	129744.017767
XDOT, KM/SEC	-0.667383122
YDOT, KM/SEC	-1.321121945
ZDOT, KM/SEC	-0.484748349

CONIC ELEMENTS AT EPOCH:

PERIGEE HEIGHT, KM	223180.32324247
ECCENTRICITY	0.73703149
INCLINATION, DEG	29.39320577
R.A. OF ASC. NODE	27.65038767
ARGUMENT OF PERIGEE, DEG	160.27937431
MINUTES TO PERIGEE	2327.53123615

CLASSICAL ELEMENTS AT EPOCH:

SEMIMAJOR AXIS, ER	136.86569426
ECCENTRICITY	0.73703149
INCLINATION, DEG	29.39320577
R.A. OF ASC. NODE	27.65038767
ARGUMENT OF PERIGEE, DEG	160.27937431
MEAN ANOMALY, DEG	353.80622205
MEAN MOTION, REV/DAY	0.01064437
PERIOD, MIN	135282.73883694

9. ACRONYMS AND ABBREVIATIONS

Table 9A. Acronyms and abbreviations in the body of the paper.

Acronym/Abbrev.	Meaning
AMOS	Advanced Maui and Optical Space Surveillance Technologies
ARG	Argument, as in Argument of Perigee
BDC	Batch UPM Differential Correction Program
DC	Differential Correction
ER	Earth Radius or Earth Radii
HGM	Herget/UPM IOD Method [5]
IAU	International Astronomical Union
IOD	Initial Orbit Determination
MPC	Minor Planet Center
MPEC	Minor Planet Electronic Circular
MST	Mountain Standard Time
NASA	National Aeronautics and Space Administration
OTA	Optical Tube Assembly
Pan-STARRS	Panoramic Survey Telescope and Rapid Response System
PPO	Pine Park Observatory
RASA	Rowe-Ackermann Schmidt Astrograph [1]
RMS	Root-Mean-Square Error
SDA	Space Domain Awareness
SO	MPC asteroid code (2020 AA was first new asteroid detected in year 2020, 2020 AB was the second)
SSA	Space Situational Awareness
UPM	Uniform Path Mechanics, a universal variables method [8, Ch. 14]
UTC	Coordinated Universal Time

Table 9B. Acronyms and abbreviations in the Appendix.

Acronym/Abbrev.	Meaning
ASC.	Ascending
BDC	Batch UPM Differential Correction Program [8, Ch. 15]
DC	Differential Correction
DDD	Day Count from January 0.0, 3 digits
ELDEC	Elevation or Declination
EPS2	Convergence Threshold, Criterion 2 [8, Ch. 15]
HH	Hours, 2 digits
ITER	Iteration Number
THETA-G	Right Accension of Greenwich at January 0.0 UTC, degrees
UPM	Uniform Path Mechanics [8, Ch. 14]
SEN	Sensor
LAT	Latitude
LONG	East longitude
MM	Minutes, 2 digits
NBR	Number
HKM	Height, km
PWRMS	Predicted Weighted RMS
RA-HRMNSEC	R.A. in Hours, Minutes, and Seconds
R.A.	Right Ascension
REV	Revolution, Orbital
RMS	Root-Mean-Square Error
SATNO	Satellite Number
SEC	Seconds
SS.SSS	Seconds SS and Fractional Seconds, SSS
TLOB	Time of Last Observation
WRMS	Weighted RMS
YY	Gregorian Year, last 2 digits of